Agomir miRNA-150-5p alleviates pristane-induced lupus by suppressing myeloid dendritic cells activation and inflammation via TREM-1 axis

Chenran Yue
Wenzhou Medical University School of Basic Medical Sciences
Sheng Gao
Wenzhou Medical University
Jianzhong Ye
Wenzhou Medical University First Affiliated Hospital: The First Affiliated Hospital of Wenzhou Medical University
Ting Zhang
Wenzhou Medical University First Affiliated Hospital: The First Affiliated Hospital of Wenzhou Medical University
Zhouhang Xing
Wenzhou Medical University School of Basic Medical Sciences
Yuanyuan Xie
Wenzhou Medical University School of Basic Medical Sciences
Hengrong Qian
Wenzhou Medical University
Xueyin Zhou
Wenzhou Medical University
Shuting Li
Wenzhou Medical University
Anni Yu
Wenzhou Medical University
Liangxing Wang
Wenzhou Medical University First Affiliated Hospital: The First Affiliated Hospital of Wenzhou Medical University
Chunyan Hua (huachunyan@wmu.edu.cn)
Wenzhou Medical University https://orcid.org/0000-0001-7957-6106

Research Article

Keywords: SLE, mDCs, Lupus, TREM-1 signaling pathway, miR-150-5p

Posted Date: February 22nd, 2023

DOI: https://doi.org/10.21203/rs.3.rs-2595324/v1

Title: Agomir miRNA-150-5p alleviates pristane-induced lupus by suppressing myeloid dendritic cells activation and inflammation via TREM-1 axis

Running title: Agomir miRNA-150-5p alleviates lupus by targeting TREM-1

Chenran Yue[1] · Sheng Gao[2] · Jianzhong Ye[3] · Ting Zhang[4] · Zhouhang Xing[1] · Yuanyuan Xie[1] · Hengrong Qian[5] · Xueyin Zhou[5] · Shuting Li[5] · Anni Yu[5] · Liangxing Wang[6] · Jianguang Wang[1] · Chunyan Hua[1]

Addresses:

[1]School of Basic Medical Sciences, Wenzhou Medical University, Wenzhou 325035, Zhejiang Province, China.

[2]Laboratory Animal Center, Wenzhou Medical University, Wenzhou 325035, Zhejiang Province, China.

[3]Department of Clinical Laboratory, The First Affiliated Hospital of Wenzhou Medical University, Wenzhou 325035, Zhejiang Province, China.

[4]Department of Rheumatology, The First Affiliated Hospital of Wenzhou Medical University, Wenzhou 325035, Zhejiang Province, China.

[5]School of the 2nd Clinical Medical Sciences, Wenzhou Medical University, Wenzhou 325035, Zhejiang Province, China.

[6]Key Laboratory of Heart and Lung, Division of Pulmonary Medicine, The First Affiliated Hospital of Wenzhou Medical University, Wenzhou 325035, Zhejiang Province, China.

Chenran Yue, Sheng Gao, Jianzhong Ye and Ting Zhang contributed equally to this work.

Correspondence:

✉ **Chunyan Hua** huachunyan@wmu.edu.cn

✉ **Jianguang Wang** wz_wjg@163.com

✉ **Liangxing Wang** wangliangxing@wzhospital.cn

Abstract

Triggering receptors expressed on myeloid cell-1 (TREM-1) has been shown to participate in inflammatory autoimmune diseases. Nevertheless, the detailed underlying mechanisms and therapeutic benefits remain elusive, especially in myeloid dendritic cells (mDCs) and systemic lupus erythematosus (SLE). In this study, we screen TREM-1 as one of the hub genes closely correlated with the progression of SLE and identify soluble TREM-1 (sTREM-1) in serum as a valuable diagnostic biomarker for SLE. Moreover, activation of TREM-1 by its agonist promotes activation and chemotaxis of mDCs and increases production of inflammatory cytokines and chemokines, showing higher expression of IL-6, TNF-α and MCP-1. Disorders of epigenetic processes including non-coding RNA give rise to SLE, resulting in complicated syndromes. Herein, we show that lupus mice display a unique miRNA signature in spleen, among which miR-150 is the most significantly expressed miRNA that targeting TREM-1 compared with wild type group. Transfection of miRNA-150-5p mimics directly suppresses the expression of TREM-1 by binding to its 3' UTR. Our in vivo experiments first indicates that administration of miR-150-5p agomir effectively ameliorates lupus symptoms. Intriguingly, miR-150 inhibits the over activation of mDCs through TREM-1 signal pathway in lymphatic organs and renal tissues. Overall, TREM-1 represents a potentially novel therapeutic target and we identify miR-150-5p as one of the mechanisms to alleviate lupus disease, which is attributable for inhibiting mDCs activation through TREM-1 signaling pathway.

Keywords: SLE, mDCs, Lupus, TREM-1 signaling pathway, miR-150-5p

Introduction

Systemic lupus erythematosus (SLE) is a life-threatening autoimmune disorder characterized by massive production of autoantibodies against nuclear antigens along with immune complex (IC) deposition leading to inflammatory damage of multiple organs [1, 2]. Patients with SLE display distinct clinical manifestations, and among them, lupus nephritis (LN) is the most feared which is associated with poor clinical outcome [3]. The current standard treatment of lupus is still unsatisfactory and often associates with severe side effects [2, 4, 5]. Thus, there is an urgent need to elucidate the key immune mechanism in order to identify evaluated biomarkers and effective therapeutic targets.

Although the etiology of SLE remains largely unknown, abnormalities in the innate and adaptive immune systems all participate in the occurrence and development of SLE. Over-activated T and B lymphocytes are the main effector cells which mediate aberrant inflammatory responses and autoantibodies production and therefore they are considered as the main therapeutic targets in the treatment of SLE [6-8]. In the past few decades, researchers shifted the focus to a pivotal immunomodulator: dendritic cells (DCs) due to their ability to derive immune activation or establish and maintain immune tolerance [9-11]. One crucial mechanism underlying SLE is the significant alternations of DCs in frequencies, phenotypes and functions. Evidence from patients with SLE and mice with lupus-like syndromes suggest that the abnormal activation of DCs including the increased expression of costimulatory molecules (CD40, CD80, and CD86), major histocompatibility complex (MHC) molecules and chemokine receptors, was associated to the occurrence of SLE immune disorders [12-14]. As the most potent professional antigen-presenting cells (APCs), dysfunction of DCs, especially myeloid DCs (mDCs), results in overactivation of autoreactive T and B lymphocytes and they play critical roles in the onset, amplification and perpetuation of SLE [11]. Therefore, unraveling the molecular mechanisms involved in the dysregulation of DCs will provide clinical advantages for SLE therapy.

Triggering receptor expressed on myeloid cells-1 (TREM-1), a novel innate immune receptor, is widely expressed on neutrophils, DCs, and macrophages. Previous studies indicated that TREM-1 was closely linked to various infections, as well as acute and chronic noninfectious inflammatory disorders [15-18]. Moreover, our Review has highlighted the characteristics and pivotal roles of TREM-1 in autoimmune diseases [19]. TREM-1 signal pathway can initiate inflammation or amplify inflammatory responses by synergizing with Toll like receptors (TLRs) and/or nucleotide-binding oligomerization domain (NOD)-like receptors (NLRs) [20, 21]. Furthermore, activation of TREM-1 in human monocytes increased the expression of co-stimulatory molecules (CD40 and CD86) and MHC-II molecules leading to the differentiation of monocytes into DCs with subsequent improvement of their ability to present antigens and elicit T cell responses [22]. Our previous study provided the first evidence that the surface expression of TREM-1 on myeloid DCs from spleen of MRL/*lp*r mice was enhanced compared to control group [23]. Thus, modulation of TREM-1 signal pathway seems to be a promising strategy to treat SLE. However, the precise function of TREM-1 and its downstream factors in SLE particularly in orchestrating phenotypic and functional properties of mDCs is largely unknown. Also, the epigenetic factors that modulate TREM-1 signal pathway in mDCs during the development of lupus have not been well clarified.

In the present study, differentially expressed genes (DEGs) between patients with SLE and healthy individuals were analyzed by four mRNA microarray datasets from Gene Expression Omnibus (GEO). TREM-1 was identified as a hub gene closely correlated with the progression of SLE. The validation experiment of clinical samples also confirmed that TREM-1 is highly expressed in PBMCs of SLE patients. Further analysis of soluble TREM-1 (sTREM-1) in serum indicated that sTREM-1 might serve as a valuable diagnostic biomarker for SLE. The effects of TREM-1 cascade on mDCs phenotype and

function were investigated. Furthermore, we found that miRNA-150 is an important epigenetic regulator that can directly bind to the 3'-UTR region of TREM-1 to directly inhibit its expression. In lupus like murine model, miR-150-5p agomir treatment ameliorated organ damage and autoimmune responses, which were closely associated with the inhibition of TREM-1 signal pathway and the activation of mDCs *in vivo*. Therefore, our results reveal an unsuspected role of TREM-1 in SLE and demonstrate that regulation of TREM-1 signal pathway by miRNA-150 can be used as an effective means to alleviate lupus progression.

Materials and methods

Ethics statement

Informed consent was obtained from all human participants. All experimental methods in the current study were approved by the research committee at Wenzhou Medical University. All experiments were carried out in accordance with guidelines from the research committee at Wenzhou Medical University (Certificate No. SYXK- (Zhejiang, China) (2018-0017)). All experiments using mice were approved by the Institutional Animal Care and Use Committee at Wenzhou Medical University (Animal Welfare Assurance). The study protocol was approved by the Clinical Research Ethics Committees of the First Affiliated Hospital of Wenzhou Medical University.

Human subjects

This study was followed in accordance with the Helsinki Declaration. 23 healthy controls (HCs) and 64 patients with SLE were enrolled from the First Affiliated Hospital of Wenzhou Medical University from May 2020 to December 2022. All participants have signed the informed Consent. Serum from 64 SLE patients and 23 HCs were collected in the First Affiliated Hospital of Wenzhou Medical University. The clinical features of SLE and HC cases were displayed in Supplementary Table S1. The patients fulfilled the American College of Rheumatology revised criteria for the classification of SLE [24]. SLE disease activity index 2000 (SLEDAI-2K) was determined at the time of blood sampling [25].

Mice

Specific pathogen-free 4-6 weeks old C57BL/6 mice were purchased from the Beijing Vital River Laboratory Animal Technology Co., Ltd. The animals were maintained on standard rodent chow and water. All mice were given at least 1 week to acclimate to their surroundings prior to use. Pristane induced murine lupus: female BALB/c mice (6–8 weeks old) were bought from the Beijing Vital River Laboratory Animal Technology Co., Ltd. and were housed in a pathogen-free condition in a 12 h light and dark cycle. All procedures involved in mice were approved by the institutional guidelines for animal care and used based the Animal Care Committee at Wenzhou Medical University. All animals were acclimatized for 2 weeks before experiments, the mice were injected with 0.5 mL of pristane (Sigma) by intraperitoneal injection, which defined as 0 month.

Cell culture

DCs were generated from femur and tibia bone marrow (BM) progenitor cells of wild type C57BL/6 mice. Briefly, BM cells were treated with red blood cell lysing buffer and washed twice with PBS. Cells were seeded into 12-well plates at a density of 1×10^6 cells/mL with complete medium (RPMI 1640 supplemented with 10% heat-inactivated fetal bovine serum, 10 ng/mL recombinant GM-CSF, and 10 ng/mL recombinant IL-4) (PeproTech). Half of the culture medium was replaced with fresh medium every 2 days. After 7 days of culture, non-adherent and loosely adherent cells were harvested and transferred into appropriate plates as needed according to further experiments. All cultures were incubated at 37 °C in 5% humidified CO_2.

Data source

The gene expression matrixes were obtained from microarray datasets GSE144390, GSE50772, GSE20864 and GSE45291 which were available at the Gene Expression Omnibus (GEO) database (www.ncbi.nlm.nih.gov/geo/). “Systemic lupus erythematosus” was used as a keyword for searching. The GSE144390(containing 3 SLE PBMCs samples and 3 health control PBMCs samples) was based on the GPL6244 platform (Afymetrix Human Gene 1.0 ST Array), the GSE50772 (containing 61 SLE PBMCs samples and 20 health control PBMCs samples) was based on the GPL570 platform (Affymetrix Human Genome U133 Plus 2.0 Array), the GSE20864 (containing 21 SLE peripheral blood samples and

45 health control peripheral blood samples) was based on the GPL1291 platform (Hitachisoft AceGene Human Oligo Chip 30K 1 Chip Version) and the GSE45291 (containing 292 SLE whole blood samples and 20 control whole blood samples) was based on the GPL13158 platform (Affymetrix HT HG-U133+ PM Array Plate). The above datasets were analyzed by GEO2R to obtain corresponding DEGs. The "ggplot2" R package was then employed to make volcano and heat maps of differential genes. Finally, the corresponding intersection and Wayne diagram was obtained by Venny (http://bioinfogp.cnb.csic.es/tools/venny/).

GO and KEGG analysis

The DEGs obtained by intersection of four datasets were enriched in Gene Ontology (GO) biological process (BP), GO cellular component (CC), and GO molecular function (MF), which was performed by the "clusterProfiler" R package. The Visualization results of GO analysis were presented by "ggplot2" R package. Then the DEGs were introduced into the FunRich3.1.3 (functional enrichment analysis tool) (http://www.funrich.org/) for Kyoto Encylopaedia of Genes and Genomes (KEGG) pathway analysis. The results were presented in a bar chart.

Hubgene identification and analysis of PPI network

Intersection genes that were upregulated in each dataset were put into the "STING" (https://string-db.org/) database for protein-protein interaction (PPI) network. Cytoscape v3.9.1 and the CytoHubba plugin (version 0.1) were used to screen the hub genes. The top 15 hub genes were obtained based on the filtering algorithm (closeness).

Screening of miRNAs targeting TREM-1

TargetScan(http://www.targetscan.org/vert_72/),miRNAMap(http://mirnamap.mbc.nctu.edu.tw/), miRWalk (http://mirwalk.umm.uni-heidelberg.de/) were used to predict differentially expressed miRNA in different species of targeting TREM-1. Venny (https://bioinfogp.cnb.csic.es/tools/venny/) is used to obtain the intersections of a Venn diagram. Intersection between differentially expressed TREM-1-targeting miRNAs in different species. Finally, miRNAs that targeting TREM-1 were identified.

RNA isolation and quantitative PCR

Total RNA was extracted using the Trizol reagent according to the recommendations of the manufacturer (Invitrogen). RNA concentrations were quantified by spectrophotometer at 260 nm. One microgram of RNA was then reverse-transcribed in a 20 μL system using a Revert Aid First-Strand cDNA Synthesis kit (Vazyme). Subsequently, 1 μL of complementary DNA was used as the template for the PCR, which used a 2 X Taq Enzyme Mix kit (Vazyme). The sequences of the primers were showed in Supplementary Table S2.

miRNA quantification: Bulge-loop™ miRNA RT-qPCR Primer Sets (one RT primer and a pair of qPCR primers for each set) specific for miR-15a, miR-15b, miR-16, miR-122, miR-20b, miR-532, miR-93 and miR-150 are designed by RiBoBio (Guangzhou, China). To determine the quantity of mature miRNA, the specific TaqMan MicroRNA Assay kit (RiBoBio) was used, and the expression levels were normalized to small nuclear RNA U6. Relative expression levels were calculated using the $2^{-\Delta\Delta ct}$ method.

Western blot

DCs were washed with cold PBS and lysed in ice-cold buffer containing protease and phosphatase inhibitors. After incubation for 30 min at 4 °C, cellular debris was removed by centrifugation and protein-containing supernatants were collected. Total protein concentration was determined using the BCA protein assay (Beyotime Biotechnology) according to the manufacturer's recommendation. Equal amounts of the protein-containing supernatants were mixed with 1×loading buffer and heated at 100°C for 5 min. Samples were electrophoresed in 10% SDS-PAGE and transferred to a polyvinylidene

difluoride membrane (Roche, Germany) by electroblotting. Membrane was blocked with 5% bovine serum albumin (BSA) for 2 h, washed briefly, incubated overnight with primary antibodies against rabbit anti-mouse phospho-STAT3 (9134, Cell Signaling Technology), phospho-IκB-α (AF2002, Affinity), IκB-α (AF5002, Affinity), STAT3 (4904, Cell Signaling Technology), GAPDH mAb (AF7021, Affinity) and mouse anti-TREM-1 antibody (DF6091, Affinity) at 1:1000 dilutions in antibody dilution buffer (5% BSA in TBST) with gentle shaking at 4℃. Blots were washed with TBST (3 times, 10 min/wash) and incubated for 2 h at room temperature with HRP-conjugated secondary antibodies (S001, Affinity). After washing, the proteins were detected with enhanced chemiluminescence HRP substrate system (Millipore), and the bands were visualized by gel imaging system (Tanon). The results represent at least three independent experiments. Quantification of band intensities was performed with Image J software (National Institutes of Health).

Flow cytometry

For DCs stimulation, 10 μg/mL of control IgG or anti-TREM-1 antibody (R&D Systems) were added in 6 well plate and were collected after 24 h. Meanwhile, 100 ng/mL LPS (InvivoGen) were also added in 6 well plate as positive control. DCs were washed twice in FACS medium phosphate buffered saline (PBS) containing 1% FCS and 0.1% NaN_3. Then, the cells were incubated for 30 min at 4°C with antibodies according to the standard procedure. A single-cell suspension was prepared from dissected spleens. Red blood cell (RBC) lysis was achieved using BD FACS Lysing solution as per manufacturer's instructions. Splenocytes were resuspended in PBS with 1% (vol/vol) FCS and labeled with the appropriate antibodies or isotype control. Monoclonal antibodies against the following antigens were used: CD11c-PE (12-0114-82, Invitrogen), MHC-II-APC (17-5321-82, Invitrogen), CD40-FITC (11-0402-82, Invitrogen), CCR7 (1633498, R&D Systems) and TREM-1-FITC (1564352, R&D Systems). To identify the expression of CD40 and TREM-1 on murine splenic cDCs, cells were gated on $CD11c^+$ MHC-II^+ and analyzed CD40 and TREM-1 expression. An isotype control was used for each antibody. The data were analyzed with FlowJo software.

Transfection of miRNA mimics and negative control

The miRNAs specific to miR-150-5p mimics and the negative control (NC) were designed and synthesized by manufacturer (RiBoBio, Guangzhou, China). Transfection of DCs with miRNA mimics and negative control were optimized utilizing lipofectamine 3000 (L3000015, Invitrogen) according to the recommendations of the manufacturer. The transfection efficiency was at least 80%. DCs were transfected with the miR-150 mimics and negative control at a final concentration of 200 nmol/L, respectively. Cells were harvested for 24h after miRNA transfection.

Chemotaxis activity analysis

Transwell chambers was used to detect the migration ability of DCs [26, 27]. DCs treated were collected and resuspended with chemotaxis medium (RPMI-1640 containing 1% BSA and 25 mM HEPES) to adjust cell density to 1×10^6/mL. Cell suspension (100 μL) was cultured in the upper chambers of transwell-24 pore plate, and 600 μL, CCL19 (200 ng/mL, PeproTech) was added to lower chambers. After incubation for 3 h at 37℃, migrated cells were harvested from the lower chambers. They were washed with cold PBS containing 2% FBS, and they were labeled with surface antibody CD11c-PE for 30 min on ice in dark. $CD11c^+$ cells were counted by flow cytometry.

Luciferase reporter assays

HEK293T cells were co-transfected with the pmirGLO plasmid containing the wild type or mutated TREM-1 3′UTR (Promega) and miR-150-5p mimics or negative controls using Lipofectamine 3000 (L3000015, Invitrogen) in 96-well plates. Firefly and Renilla luciferase activities were measured 24 h

after transfection using a dual luciferase reporter assay kit (Promega) following the manufacturer's protocol. Renilla luciferase activity values were used for normalization.

miR-150-5p agomir treatment in pristane induced-lupus mice model

Three groups were defined in the experiment as Ctrl group (control mice), miR-150-5p agomir group (pristane-induced lupus mice treated with miR-150-5p agomir), and NC-agomir group (pristane-induced lupus mice treated with NC-agomir). When the mice injected with pristane grew to 5 months, they were treated with miR-150-5p agomir and agomir negative control. The miR-150-5p agomir and agomir negative control were synthesized by RiboBio (Guangzhou, China) (n = 4 per group). Each mouse received a tail vein injection of either miR-150-5p agomir or agomir negative control, at a dose of 20 nmol in 0.2 mL saline every twice a week for 4 weeks and sacrificed 48 h after the last injection. Serum, spleens, lymph nodes and kidneys were harvested. The onset of disease progression in lupus mice was monitored by assessment of proteinuria, determined using BCA Protein Assay Kit (P0010S, Beyotime Biotechnology), simultaneously, the weight changes of lupus mice also regularly recorded.

ELISA

The serum of patients and samples was analyzed for sTREM-1 with ELISA kits (JL18244-96T, Solabio) according to manufacturer's instruction. The mice serum levels of total IgG (46639M1, MeiMian) and ds-DNA (46273M1, MeiMian) were determined by performing a sandwich ELISA based on the manufacturer's published protocols. The absorbance at 450 nm was determined using a micro-ELISA plate reader. Each sample was run in duplicate and averaged.

Renal histopathology and immunofluorescence

Whole kidneys were fixed in 10% buffered formalin overnight, dehydrated and embedded in paraffin. For histological examination, kidney samples were taken after routine fixation and paraffin embedding of the tissues. Sections 4 μm thick were cut and stained with hematoxylin-eosin (HE) and periodic acid-Schiff (PAS) staining (G1281-4, Solarbio). Glomerular pathology scores were determined by individuals blinded to the genotypes of the animals. Briefly, the severity of glomerulonephritis was graded on a 0–4 scale as follows: 0, normal; 1, mild, or early proliferative; 2, multifocal proliferative with increased matrix; 3, diffuse proliferative; 4, strong intracapillary proliferation, extensive sclerosis/crescents [28]. Images were captured under a light microscope (Leica). For immunofluorescence： kidneys were embedded in Tissue-Tek O.C.T. (Sakura Finetek) and frozen at −80 °C for further immunofluorescence. Acetone fixed sections were blocked for 1 h by goat serum working solution (Beijing Zhongshan Jinqiao Biotechnology Co., Ltd.). Kidney frozen sections were stained with the following antibodies: C3-FITC (sc-58926, Santa) and IgG-FITC (SA00013, Proteintech) overnight at 4°C. After rinsing, nuclei were counter stained with DAPI (P0131, Beyotime Biotechnology). Images were acquired using confocal microscopy (Nikon). The immunofluorescence (IF) intensity within the peripheral glomerular capillary walls and mesangial region were scored on a scale from 0 to 3 (0 = none; 1 = weak; 2 = moderate; 3 = strong) [29]. At least 4 glomeruli/section were analyzed. The integrated density of IgG and C3 deposits was evaluated by assessing Image J software on a semi-quantitative scale.

Statistical analysis

The data were presented as mean ± SD from three independent experiments. Statistical analysis was performed using the student's t-test for between group comparisons or one-way ANOVA for multiple group comparisons in GraphPad Prism 6.0 (GraphPad Software, La Jolla, CA, USA). Differences were considered significant when $p < 0.05$.

Results

Screening of DEGs and functional correlation analysis

Based on the high throughput analysis, differentially expressed genes (DEGs) in four microarray datasets containing SLE patients and HCs were screened with two-group comparisons ($p < 0.05$). A total of 1179 (up-regulated 708 and down-regulated 471 genes), 8475 (up-regulated 3924 and down-regulated 4551 genes), 10550 (up-regulated 4627 and down-regulated 5923 genes) and 3096 (up-regulated 1389 and down-regulated 1707 genes) DEGs from GSE144390, GSE50772, GSE45291 and GSE20864 were identified respectively (Fig. 1A, Supplementary Table S3). Among them, 111 DEGs overlapped in the four datasets (Fig. 1B) and were performed by functional enrichment analysis further. The results showed that these DEGs were categorized into three function groups: cellular component group, molecular function group, and biological process group. In the biological process group, the most significantly enriched GO term of the 111 common DEGs were significantly enriched in some biological processes related to SLE, such as cytokine-mediated, type I IFN and pattern recognition receptor signaling pathways (Fig. 1C, Supplementary Table S4). Results of the KEGG analysis indicated that cytokines and type I IFN mediated responses were most relevant to the pathogenesis of SLE (Fig 1D, Supplementary Table S5). We conducted more in-depth screening in order to further find out highly expressed genes closely related to these pathways. Based on the integration analysis, 26 significantly common up-regulated genes were shown by the Venn map (Fig. 1E). The heat map showed that CHI3L1, CDA, PADI4, MNDA, and TREM-1 are the top 5 of the 26 up-regulated genes in GSE144390 (Fig. 1F). The heat maps of 26 up-regulated genes in GSE50772, GSE45291 and GSE20864 datasets were shown in supplementary Fig. S1A. The protein-to-protein interaction (PPI) network was constructed using Cytoscape and the STRING database (Supplementary Fig. S1B). Based on the closeness algorithm, the top 15 hub genes were identified using the Cytohubba plugin (Fig. 1G, Supplementary Table S6). MNDA and TREM-1, two of the top 15 linked proteins, were also among the top 5 up-regulated factors in Fig. 1F. TREM-1 is a crucial membrane receptor that controls immunological response either independently or in conjunction with other pattern recognition receptors, such as TLR2 and TLR4. It plays a pivotal role in the production of inflammatory cytokines and type I IFN. Therefore, we will further explore the important roles of TREM-1 in SLE.

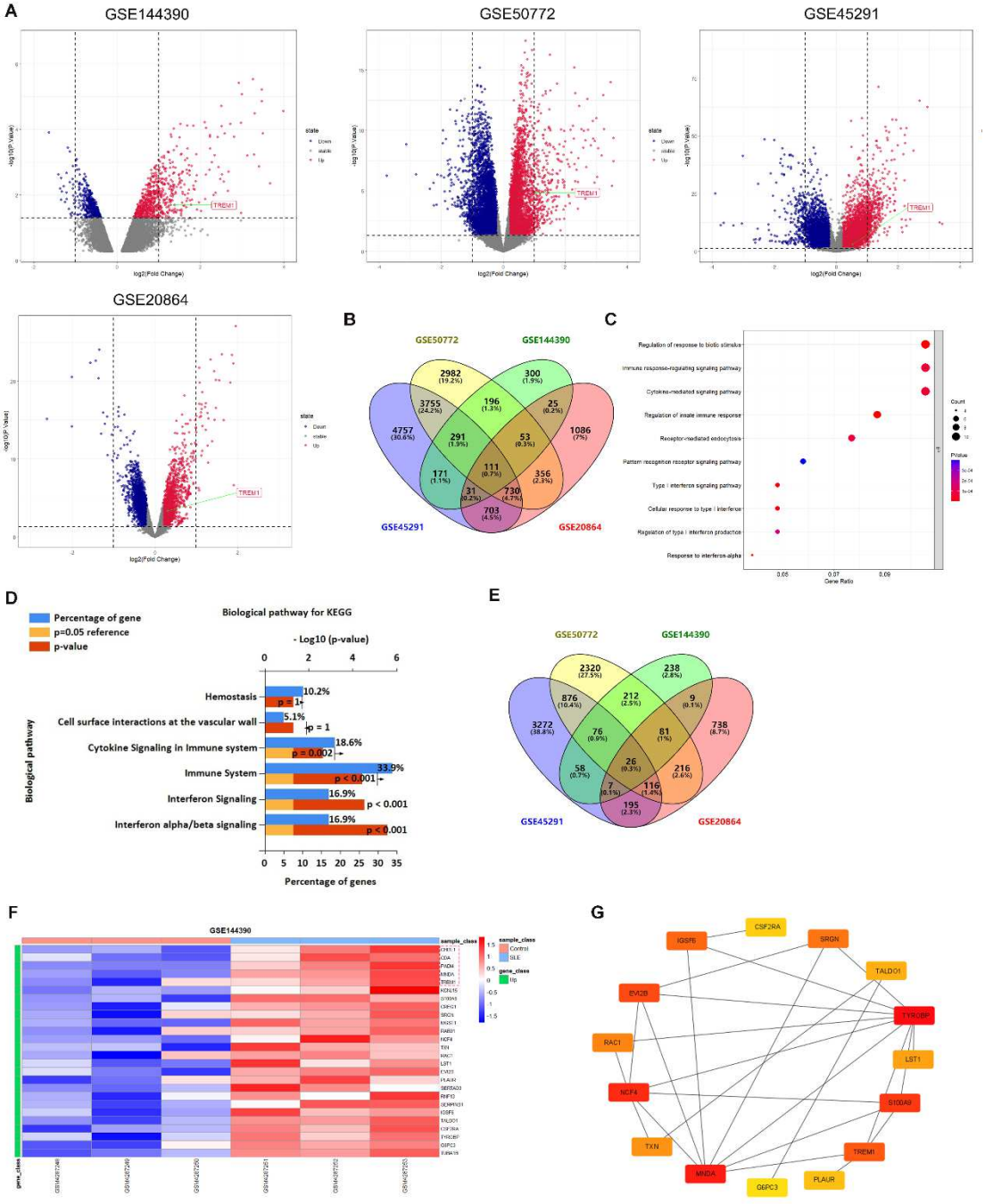

Fig. 1 Screening of DEGs in different datasets and functional correlation analysis. (**A**) The volcano plot illustrates DEGs between control and SLE after analysis of the GSE144390, GSE50772, GSE45291, and GSE20864 datasets with GEO2R. Green dots represent down-regulated expression, while red dots represent upregulated expression. (**B**) Venny is used to obtain the intersection of DEGs in four datasets, with an overlap of 111 genes. (**C**) The first 10 terms of BP in the GO enrichment map are visualized respectively. Strength of the color represents the p-value (from the lowest in green to the highest in red), and the bubble size represents the number of DEGs. (**D**) Top 6 terms of KEGG analysis in biological pathway category (Ranged by p value). (**E**) Venn diagram of the up-regulated DEGs in common between the four datasets, with an overlap of 26 genes. (**F**) Heatmap of 26 up-regulated genes in GSE144390 datasets. (**G**) Interaction network of 15 hubgenes.

Verification of sTREM-1 as a diagnostic marker for SLE

We further verified the expression characteristics and roles of TREM-1 in clinical samples of SLE (Fig. 2A). Serum sTREM-1 was significantly increased in SLE patients compared to HCs (Fig. 2B). Patients were then divided into two groups based on the median value of serum sTREM-1, and several clinical and laboratory characteristics were compared between the two groups. We found that the greater sTREM-1 group had lower serum C3 levels (Fig. 2C), and serum IgG and creatinine levels were upregulated in patients with high serum sTREM-1 (Fig. 2D, E). To test whether serum sTREM-1 could be a high-risk factor of SLE, we analyzed the correlation of sTREM-1 with some common serum markers of autoimmune diseases. Intriguingly, serum sTREM-1 levels correlated inversely with the concentration of serum C3 (Fig. 2F) while positively levels associated with IgG and creatinine levels from SLE patients. Serum IgG and creatinine levels were positively associated with serum sTREM-1 levels from SLE patients (Fig. 2G, H). Additionally, there was a positive association between the sTREM-1 levels and the SLEDAI score (Fig. 2I). TREM-1 expression in PBMCs was also significantly increased in patients with SLE (Fig. 2J-L). According to the SLEDAI score, we further divided SLE patients into inactive SLE group and active SLE groups. Serum levels of sTREM-1 in the two groups of SLE patients were higher than that in HCs, and with the progress of the disease, its expression level further increased. (Fig. 2M). The ROC curve of sTREM-1 revealed its probability as valuable biomarker with AUC of 0.9511 (95% confidence interval, 0.9097-0.9925), indicating that sTREM-1 has a high accuracy of predictive value (Fig. 2N).

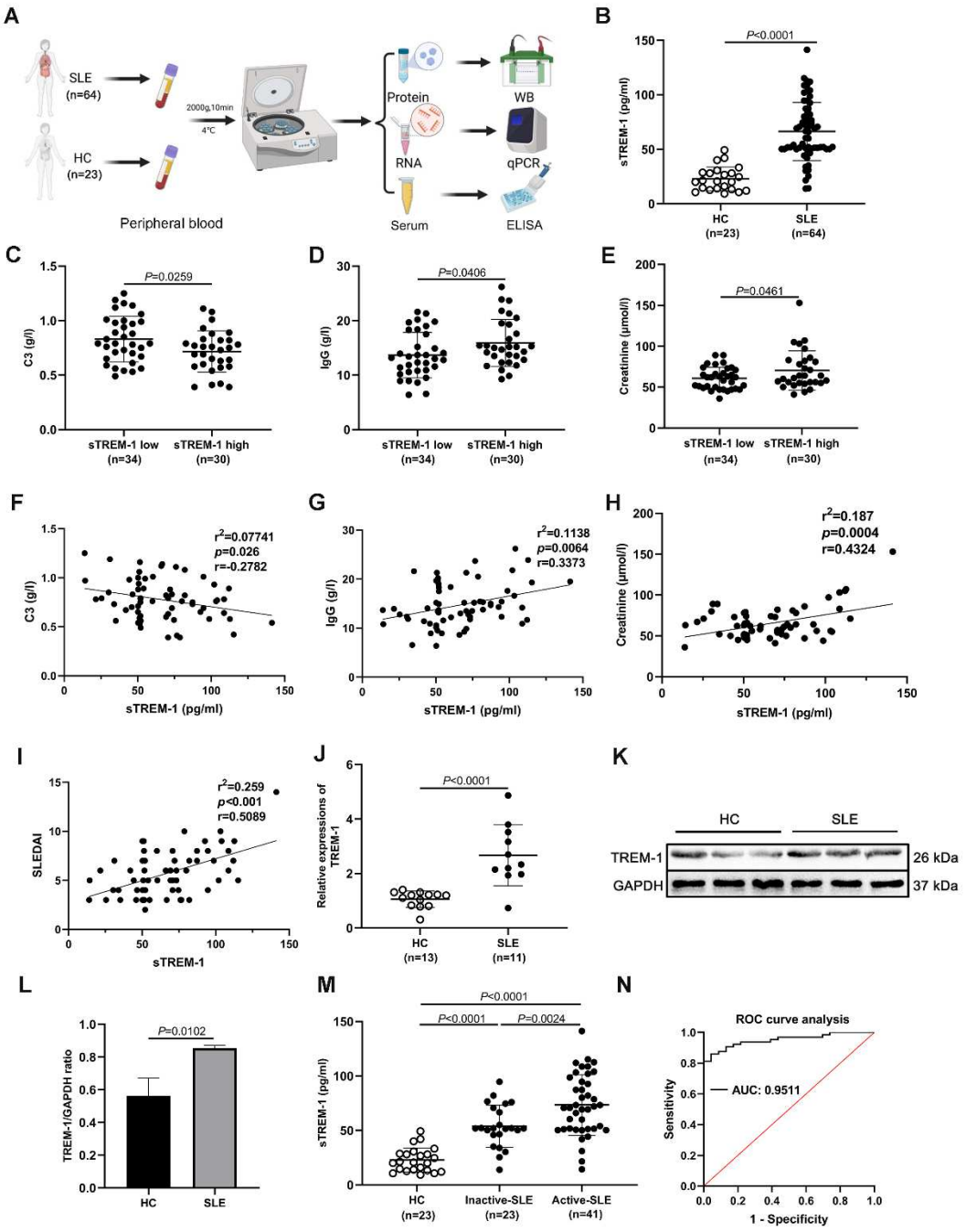

Fig. 2 Serum sTREM-1 levels are positively correlated with disease activity in lupus patients. (**A**) Schematic illustration of the experimental procedure. (**B**) Serum samples are collected from 12 to 87-year-old SLE patients (n = 64) and HCs (n = 23). The levels of sTREM-1 in serum were detected by ELISA. (**C-E**) Patients are divided into two groups based on their serum sTREM-1 levels (below or above the median value of 66.5 pg/mL). Levels of serum C3 (**C**), total IgG (**D**) and creatinine (**E**) are compared between the high and low sTREM-1 groups. (**F-H**) Correlation of sTREM-1 levels in serum from SLE patients with serum C3 (**F**), IgG (**G**) and creatinine (**H**) is analyzed. (**I**) Correlation between serum sTREM-1 levels and SLEDAI score. (**J**) qPCR analysis of the TREM-1 expression levels in PBMCs from SLE patients (n = 13) and HCs (n = 11) respectively. (**K** and **L**) Western blot analysis of the TREM-1 expression levels in PBMCs from SLE patients (n = 13) and HCs (n = 11). The protein

expression level is calculated by the ratio of protein to GAPDH. (**M**) The serum sTREM-1 levels in HCs (n = 23), patients with inactive SLE (n = 23) and patients with active SLE (n = 41) are determined by ELISA. (**N**) ROC curve analyses of sTREM-1, which show the values for AUC. All of the reactions are conducted in triplicate. Data were presented with mean ± SD. * represents $p < 0.05$, ** represents $p < 0.005$, *** represents $p < 0.001$, **** represents $p < 0.0001$.

Stimulation of TREM-1 signal pathway promotes the activation of mDCs

Our previous study confirmed the aberrant expression of TREM-1 in lupus prone mice, especially on $CD11c^+$ $MHC\text{-}II^+$ DCs (mDCs) [23]. Herein, we further examined the effect of TREM-1 signaling pathway on mDCs maturation, activation and function. It is well known that LPS can significantly promote the expression of costimulatory molecule CD40. The phenotypic analysis showed that activation of TREM-1 by its agonist synergistically enhanced this effect. Moreover, the activation of TREM-1 alone also effectively upregulated the expression of CD40 (Fig. 3A, B, E). Interestingly, stimulation of TLR4 or TREM-1 alone or in combination significantly increased the level of TREM-1 on the surface of mDCs (Fig. 3C, F). And these findings indicate that TREM-1 may serve as a novel marker to indicate the activation status of mDCs. Upon the presence of inflammatory stimuli, DCs mature and gain CCR7 expression which, by binding to its ligand CCL21 or CCL19, direct DCs to the lymph nodes for antigen presentation [30]. Therefore, we evaluated CCR7 expression on mDCs, with or without agonist of TREM-1 treatment, and their migratory capacity toward CCL19 using the transwell system. Upon agonist of TREM-1 treatment mature mDCs expressed significantly higher levels of CCR7 compared with untreated mDCs (Fig. 3D, G). Of note, the proportion of CCR7 upregulation after agonist of TREM-1 treatment alone had no significant difference compared to single LPS treatment and combined stimulation group. In addition, agonist of TREM-1 treated mDCs showed a significantly enhanced migration efficiency toward CCL19 in comparison to untreated mDCs (Fig. 3H). Next, we aimed to explore the important signal events downstream of TREM-1 pathway. Stimulation of TREM-1 promoted the phosphorylation of IκB-α and STAT3 (Fig. 3I) and increased the expression of pro-inflammatory cytokines (IL-6, TNF-α and MCP-1) (Fig. 3J-L). Collectively, these data indicate that activation of TREM-1 signaling pathway effectively regulate the activation and function of the mDCs.

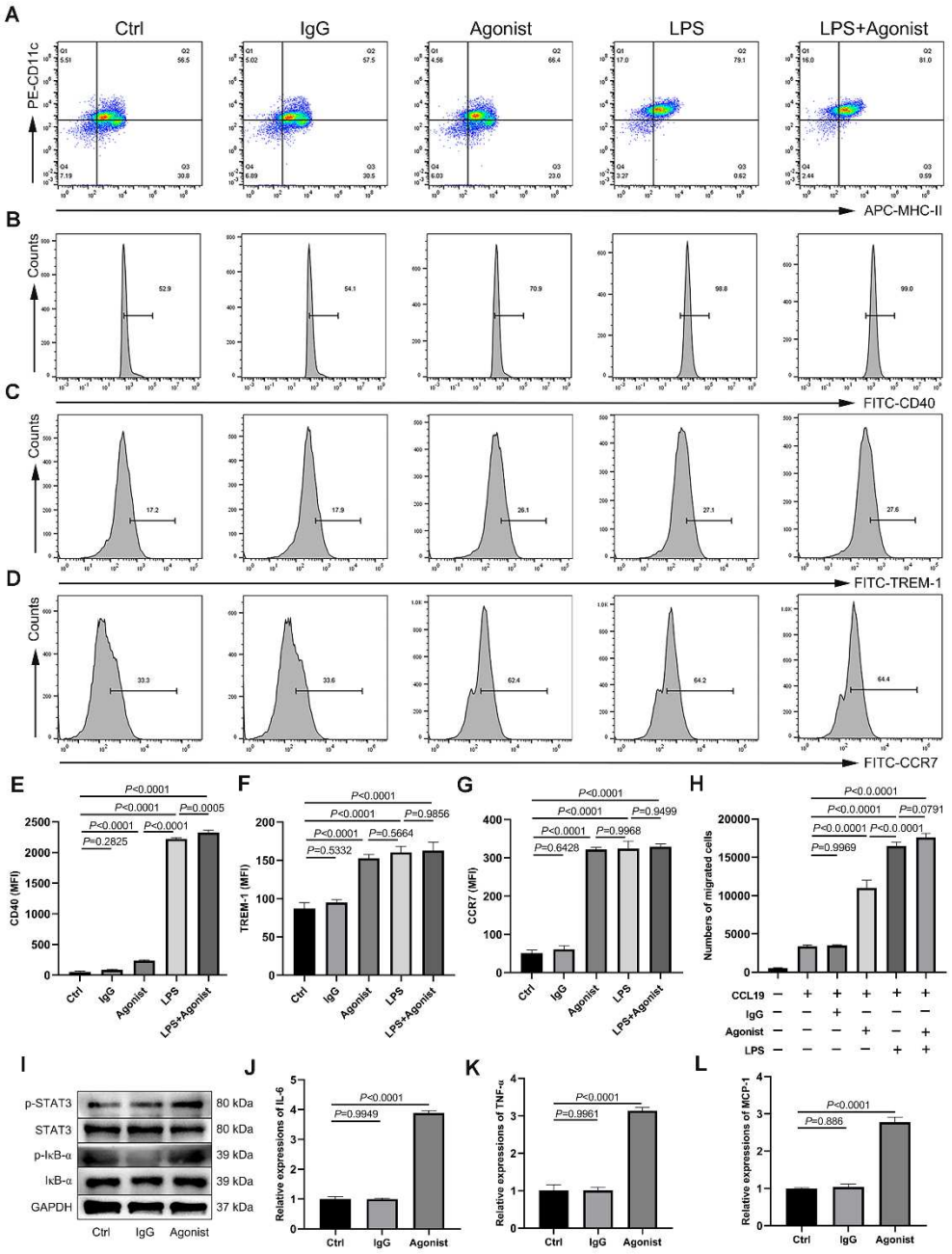
A
Ctrl
IgG
Agonist
LPS
LPS+Agonist
PE-CD11c
APC-MHC-II
B
Counts
FITC-CD40
C
FITC-TREM-1
D
FITC-CCR7
E
CD40 (MFI)
F
TREM-1 (MFI)
G
CCR7 (MFI)
H
Numbers of migrated cells
CCL19
IgG
Agonist
LPS
I
p-STAT3
STAT3
p-IκB-α
IκB-α
GAPDH
80 kDa
80 kDa
39 kDa
39 kDa
37 kDa
J
Relative expressions of IL-6
K
Relative expressions of TNF-α
L
Relative expressions of MCP-1

Fig. 3 Activation of TREM-1 signaling pathway promotes the maturation and migration mDCs. (**A** and **B**) Representative flow cytometry and quantification of CD40 MFI (**E**) in mDC cells which treated agonist of TREM-1(10 μg/mL), LPS (100 ng/mL) or LPS combined with agonist of TREM-1. DCs are treated for 24 h. (**C**) Representative flow cytometry and quantification of TREM-1 MFI (**F**) in mDC cells which treated agonist of TREM-1(10 μg/mL), LPS (100 ng/mL) or LPS combined with agonist of TREM-1. DCs are treated for 24 h. (**D**) Representative flow cytometry and quantification of CCR7 MFI (**G**) in mDC cells which treated agonist of TREM-1(10 μg/mL), LPS (100 ng/mL) or LPS combined with agonist of TREM-1. DCs are treated for 24 h. (**H**) Effect of agonist of TREM-1(10 μg/mL), LPS (100 ng/mL) or LPS combined with agonist of TREM-1 on chemotaxis ability of DCs. The migration of DCs were proved by the harvested cells from the bottom transwells chambers and counted with flow cytometry. DCs are treated for 24 h. (**I**) Western blot analysis of STAT3, phosphorylated STAT3 (p-STAT3), IκB-α and p-IκB-α expression levels in mDC cells treated with agonist of TREM-1 (10 μg/mL) for 48 h. (**J-L**) qPCR analysis of IL-6, TNF-α and MCP-1 expression levels in mDC cells treated with agonist of TREM-1 (10 μg/mL) for 24 h. All of the reactions are conducted in triplicate. Data were presented with mean ± SD. * represents $p < 0.05$, ** represents $p < 0.005$, *** represents $p < 0.001$, **** represents $p < 0.0001$.

miR-150-5p directly targets and negatively regulates TREM-1 expression

To predict miRNAs most likely to repress TREM-1 expression, we analyzed miRNA candidates by three databases: Targetscan (http://www.targetscan.org/vert_72/), miRMap (http://mirnamap.mbc.nctu.edu.tw/) and miRWalk (http://mirwalk.umm.uni-heidelberg.de/). The predicted results showed that eight common miRNAs can target the 3′ UTR of both human and murine TREM-1 (Fig. 4A). Next, the expression pattern of these miRNAs was further verified in WT and lupus like mouse. In the splenocytes of the two groups, the expression of miRNA-150 was the most significant difference (Fig. 4B). Moreover, levels of miR-150-5p also showed consistently significant decline in PBMCs of SLE patients compared with HCs (Fig. 4C). Of note, it correlated inversely with the levels of TREM-1(Fig. 4D). In order to explore whether miR-150-5p could directly target and inhibit the expression of TREM-1, miR-150-5p mimics and NC mimics were transfected into mDCs respectively (Fig. 4E). Further analysis by RT-qPCR and immunoblot showed that miR-150-5p possessed a negative effect on both the mRNA and protein levels of TREM-1 (Fig. 4F-H). Dual luciferase reporter assays demonstrated that miR-150-5p overexpression strongly suppressed the luciferase reporter gene activity of TREM-1 3′-UTR WT compared with miRNA-NC, but did not affect the activity of the TREM-1 3′-UTR mutant luciferase reporter gene, indicating that TREM-1 is a direct target of miR-150-5p (Fig. 4I, J).

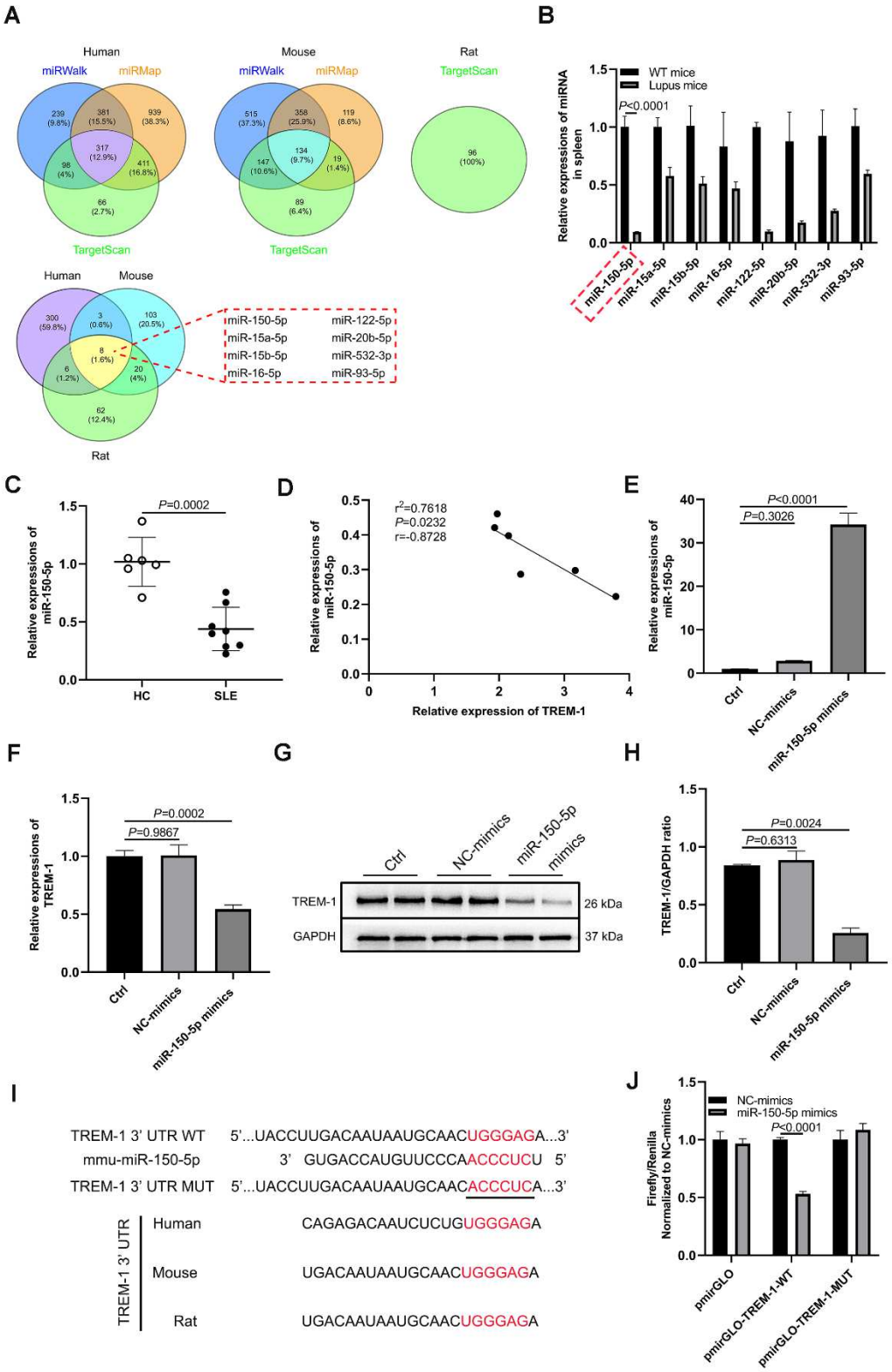
A
Human
miRWalk
miRMap
239 (9.8%)
381 (15.5%)
939 (38.3%)
317 (12.9%)
98 (4%)
411 (16.8%)
66 (2.7%)
TargetScan
Mouse
miRWalk
miRMap
515 (37.3%)
358 (25.9%)
119 (8.6%)
134 (9.7%)
147 (10.6%)
19 (1.4%)
89 (6.4%)
TargetScan
Rat
TargetScan
96 (100%)
Human
Mouse
Rat
300 (59.8%)
3 (0.6%)
103 (20.5%)
8 (1.6%)
6 (1.2%)
20 (4%)
62 (12.4%)
miR-150-5p
miR-15a-5p
miR-15b-5p
miR-16-5p
miR-122-5p
miR-20b-5p
miR-532-3p
miR-93-5p
B
WT mice
Lupus mice
P<0.0001
Relative expressions of miRNA in spleen
miR-150-5p
miR-15a-5p
miR-15b-5p
miR-16-5p
miR-122-5p
miR-20b-5p
miR-532-3p
miR-93-5p
C
P=0.0002
Relative expressions of miR-150-5p
HC
SLE
D
r²=0.7618
P=0.0232
r=-0.8728
Relative expressions of miR-150-5p
Relative expression of TREM-1
E
P<0.0001
P=0.3026
Relative expressions of miR-150-5p
Ctrl
NC-mimics
miR-150-5p mimics
F
P=0.0002
P=0.9867
Relative expressions of TREM-1
Ctrl
NC-mimics
miR-150-5p mimics
G
Ctrl
NC-mimics
miR-150-5p mimics
TREM-1
GAPDH
26 kDa
37 kDa
H
P=0.0024
P=0.6313
TREM-1/GAPDH ratio
Ctrl
NC-mimics
miR-150-5p mimics
I
TREM-1 3' UTR WT 5'...UACCUUGACAAUAAUGCAACUGGGAGA...3'
mmu-miR-150-5p 3' GUGACCAUGUUCCCAACCCUCU 5'
TREM-1 3' UTR MUT 5'...UACCUUGACAAUAAUGCAACACCCUCA...3'
TREM-1 3' UTR
Human CAGAGACAAUCUCUGUGGGAGA
Mouse UGACAAUAAUGCAACUGGGAGA
Rat UGACAAUAAUGCAACUGGGAGA
J
NC-mimics
miR-150-5p mimics
P<0.0001
Firefly/Renilla Normalized to NC-mimics
pmirGLO
pmirGLO-TREM-1-WT
pmirGLO-TREM-1-MUT

Fig. 4 The expression of TREM-1 is directly repressed by miR-150-5p. (**A**) Intersection of miRNAs that can target TREM-1 in TargetScan, miRMap and miRWalk databases. Eight miRNAs are screened. (**B**) qPCR analysis of eight miRNAs expression levels in spleen from WT and lupus mice. (**C**) qPCR analysis of miR-150-5p expression levels in PBMCs from SLE patients and HCs. Results show average and SD from SLE patients (n = 8) and HCs (n = 6). (**D**) Correlation between miR-150-5p and TREM-1. (**E**) qPCR analysis of miR-150-5p expression levels in DCs transfected with miR-150-5p or miR-NC (50 nmol). mDCs are transfected for 12 h. (**F**) qPCR analysis of TREM-1 expression levels in DCs transfected with miR-150-5p or miR-NC (50 nmol). DCs are transfected for 12 h. (**G** and **H**) Western blot analysis of TREM-1 expression levels in DCs transfected with miR-150-5p or miR-NC (50 nmol). DCs are transfected for 48 h, with GAPDH used as a loading control. The protein expression level is calculated by the ratio of protein to GAPDH. (**I**) Predicted binding sites for miR-150-5p in the 3′ UTR of TREM-1. (**J**) HEK293T cells ($1x10^6$) are transfected with the control construct (pmirGLO), or a construct encoding the wild-type TREM-1 3′ UTR or mutated TREM-1 3′ UTR (mutant), in addition to the miR-150-5p mimic. After 24 h, luciferase activity in HEK293T cells lysates is detected. All of the reactions are conducted in triplicate. Data were presented with mean ± SD. * represents $p < 0.05$, ** represents $p < 0.005$, *** represents $p < 0.001$, **** represents $p < 0.0001$.

miR-150-5p agomir treatment ameliorates organ damage and autoimmune responses in pristane-induced lupus mice

We next assessed the effects of miR-150-5p on lupus mice *in vivo*. Pristane-induced lupus mice were injected with 20 nmol miR-150-5p agomir or NC-agomir every 3 days for 4 weeks to examine whether systemic administration of miR-150-5p agomir could rescue the organ damage in lupus mice (Fig. 5A). When compared to control group, NC-agomir group showed severe splenomegaly and lymphadenopathy, while treatment with miR-150-5p agomir significantly decreased the spleen and lymph node index (Fig. 5B, C). The high levels of serum antibodies contribute to the pathogenesis of SLE [31, 32]. Therefore, we detected the serum levels of total IgG and anti-dsDNA of each group. As shown in Fig. 5D and E, we found that the serum total IgG and anti-dsDNA levels in NC-agomir group significantly enhanced compared with control group. However, the levels of total IgG and anti-dsDNA in miR-150-5p agomir-treated group were lower than those in NC-agomir group. To further confirm the effect of miR-150-5p agomir on lupus nephritis, kidney section histopathology was detected. HE and PAS staining showed that inflammatory cells infiltrations and the mesangial matrix diffuse expansion decreased in miR-150-5p agomir-treated group compared with NC-agomir group (Fig. 5F). Meanwhile, reduced glomerular depositions of IgG and C3 were observed in miR-150-5p agomir-treated group compared with NC-agomir group (Fig. 5G). Collectively, these data suggest that miR-150-5p agomir significantly alleviates organ damage and disease progression in pristane-induced lupus mice.

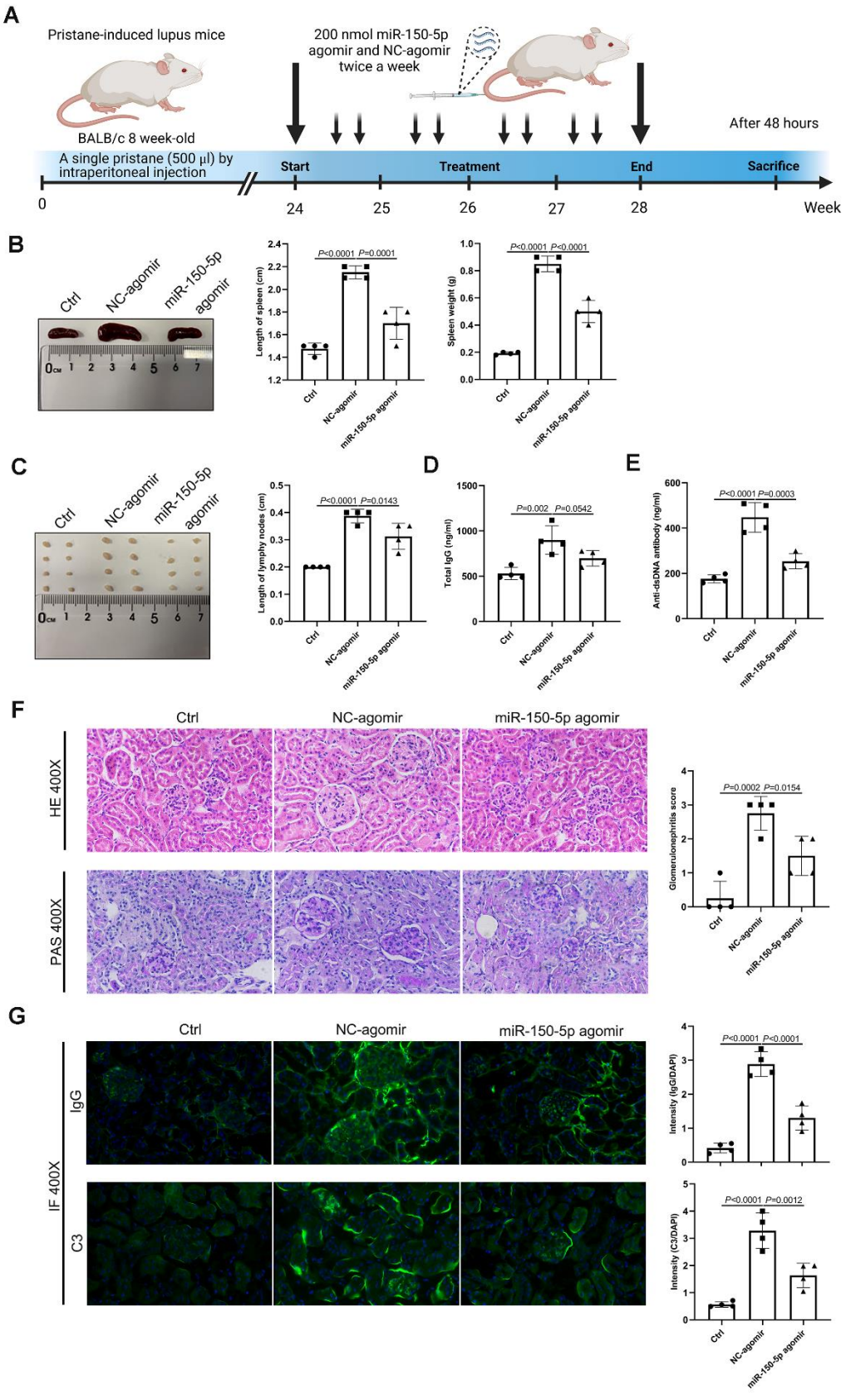
A
Pristane-induced lupus mice
BALB/c 8 week-old
A single pristane (500 μl) by intraperitoneal injection
200 nmol miR-150-5p agomir and NC-agomir twice a week
After 48 hours
Start
Treatment
End
Sacrifice
0
24
25
26
27
28
Week
B
Ctrl
NC-agomir
miR-150-5p agomir
Length of spleen (cm)
Spleen weight (g)
P<0.0001 P=0.0001
P<0.0001 P<0.0001
C
Length of lymphy nodes (cm)
P<0.0001 P=0.0143
D
Total IgG (ng/ml)
P=0.002 P=0.0542
E
Anti-dsDNA antibody (ng/ml)
P<0.0001 P=0.0003
F
HE 400X
PAS 400X
Glomerulonephritis score
P=0.0002 P=0.0154
G
IF 400X
IgG
C3
Intensity (IgG/DAPI)
P<0.0001 P<0.0001
Intensity (C3/DAPI)
P<0.0001 P=0.0012

Fig. 5 miR-150-5p agomir alleviates organ damage and immune disorders in lupus mice. (**A**) Schematic diagram of miR-150-5p agomir administration in pristane-induced lupus mice. (**B** and **C**) Spleen and lymph nodes index from Ctrl, NC-agomir and miR-150-5p agomir groups, respectively (n = 4). The statistical summary of spleens and lymph nodes in the three groups. (**D** and **E**) The levels of total IgG (**D**) and anti-dsDNA (**E**) in serum were detected by ELISA. (**F**) HE and PAS staining of kidney sections of each group (n = 4). Histological score for glomerulonephritis (score ranging from 0 to 4) were determined by HE and PAS staining. Four mice of each group of pathology score were evaluated by three pathologists. (**G**) Representative images of IgG and C3-FITC expression in kidney obtained from immunofluorescence assay. All of the reactions are conducted in triplicate. Data were presented with mean ± SD. * represents $p < 0.05$, ** represents $p < 0.005$, *** represents $p < 0.001$, **** represents $p < 0.0001$.

miR-150-5p agomir treatment supresses TREM-1 signal pathway in different organs of lupus mice

Our *in vitro* study has demonstrated that miR-150-5p negatively regulated TREM-1 expression in mDCs. Herein, we further wanted to confirm whether miR-150-5p is involved in the development of SLE by regulating TREM-1 expressed in mDCs *in vivo*. In the pathological progress of lupus, the surface expression of TREM-1 on mDCs was significantly enhanced compared with wild mice while was strongly suppressed by miR-150-5p agomir-treatment (Fig. 6A-D). In addition, we also evaluated the changes of TREM-1 in kidneys by qPCR and western blot analysis. As shown in Fig. 6E, miR-150-5p agomir treatment significantly decelerated the levels of TREM-1 compared with NC-agomir group. Although miR-150-5p agomir did not significantly down regulate the protein levels of TREM-1 in renal tissue (Fig. 6F), it could affect the major events of its downstream signal pathway. Because western blot results indicated that the phosphorylation of IκB-α and STAT3 involved in the downstream of TREM-1 signaling pathway was significantly inhibited (Fig. 6G). Finally, we aimed to verify the expression of pro-inflammatory cytokines (IL-6, TNF-α and MCP-1) which were usually elicited by activation of TREM-1 signal pathway. The data showed that IL-6 and TNF-α in miR-150-5p agomir treatment group sharply decreased compared to NC-agomir group. Of note, the expression of MCP-1 was only slightly decreased by miR-150-5p agomir, and there was no significant difference (Fig. 6H). Taken together, these results indicated that miR-150-5p agomir treatment negatively regulated the expression of TREM-1 on mDCs in lymphatic organs and inhibited the activation of TREM-1 signal axis *in vivo*.

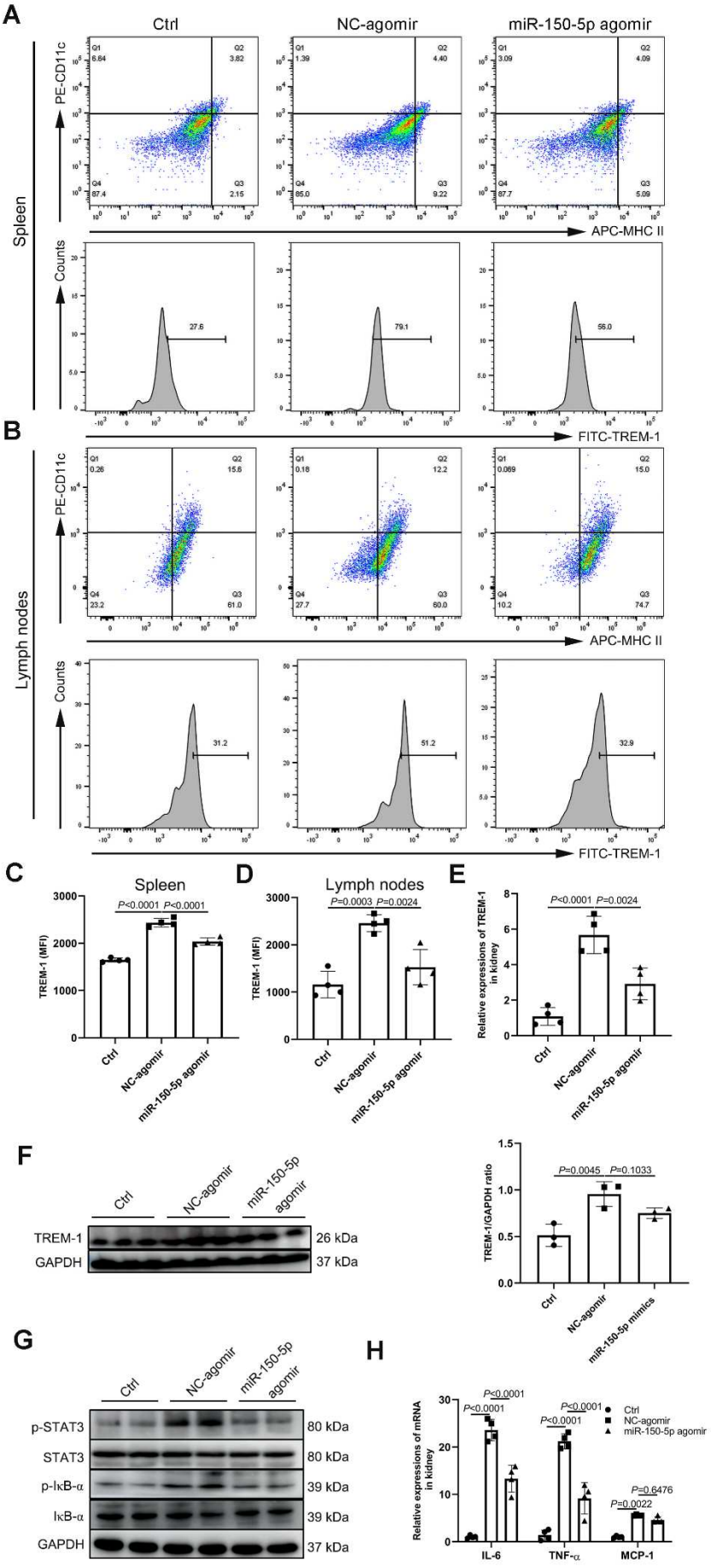
A
Ctrl
NC-agomir
miR-150-5p agomir
Spleen
PE-CD11c
APC-MHC II
Counts
FITC-TREM-1
B
Lymph nodes
C
Spleen
TREM-1 (MFI)
D
Lymph nodes
E
Relative expressions of TREM-1 in kidney
F
TREM-1
GAPDH
26 kDa
37 kDa
TREM-1/GAPDH ratio
miR-150-5p mimics
G
p-STAT3
STAT3
p-IκB-α
IκB-α
80 kDa
39 kDa
H
Relative expressions of mRNA in kidney
IL-6
TNF-α
MCP-1

Fig. 6 miR-150-5p agomir inhibits the expression of TREM-1 and its downstream pathways in lupus mice. (**A** and **C**) Representative flow cytometry and quantification of TREM-1 MFI in mDC cells of spleen (n = 4). (**B** and **D**) Representative flow cytometry and quantification of TREM-1 MFI in mDC cells of lymph nodes (n = 4). (**E**) qPCR analysis of TREM-1 expression levels in kidneys (n = 4). (**F**) Western blot analysis of TREM-1 expression levels in kidneys. The protein expression level is calculated by the ratio of protein to GAPDH (n = 3). (**G**) Western blot analysis of STAT3, phosphorylated STAT3 (p-STAT3), IκB-α and p-IκB-α expression levels in kidneys (n = 2). (**H**) qPCR analysis of the mRNA expression levels of IL-6, TNF-α and MCP-1 in the kidneys (n = 4). All of the reactions are conducted in triplicate. Data were presented with mean ± SD. * represents $p < 0.05$, ** represents $p < 0.005$, *** represents $p < 0.001$, **** represents $p < 0.0001$.

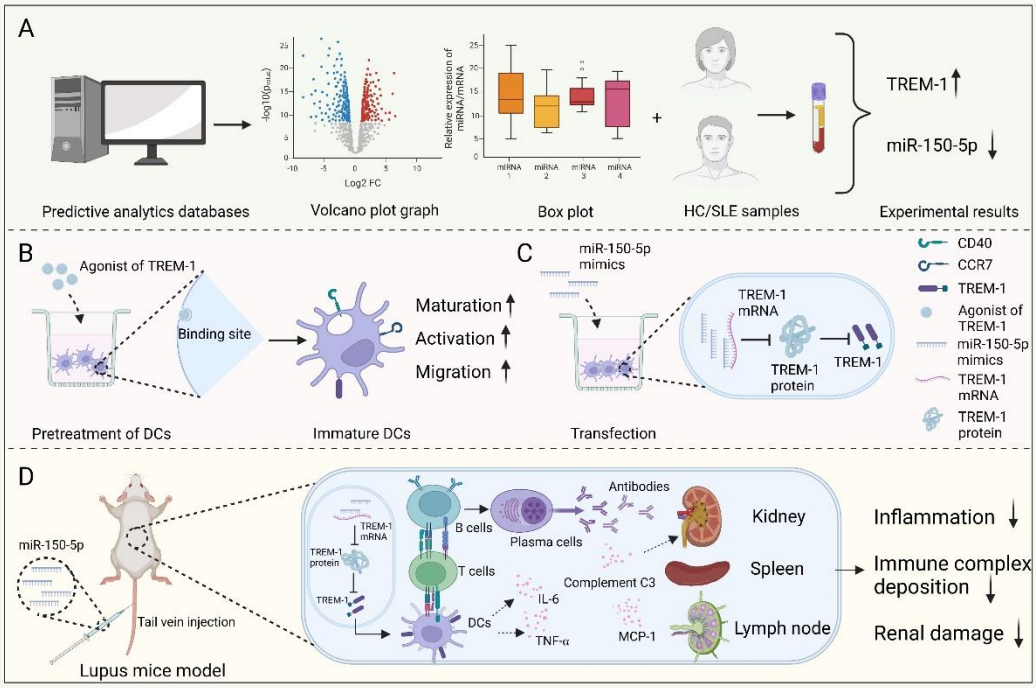

Fig. 7 The graphical abstract depicts the identification of TREM-1 and miR-150-5p expression levels in SLE patients by employing bioinformatics analysis. We further explore the effect of TREM-1 signaling pathway on mDCs maturation and function. Finally, we confirm that regulating signaling pathway of TREM-1 by miR-150-5p alleviates the manifestations of pristane-induced lupus in disease models.

Discussion

TREM-1 signaling pathway contributes to the pathology of both infectious and non-infectious inflammatory diseases [20, 33]. Given the role of TREM-1 in inflammatory conditions, an increasing number of studies focus on the key functional role of TREM-1 in different types of autoimmune diseases, which has been well discussed by our previous Review [19]. However, studies on TREM-1 in the research field of SLE are rare, and most of them are only about the detection of sTREM-1, lacking in-depth exploration of its mechanism. For instance, previous studies indicated that sTREM-1 levels in serum and plasma of SLE patients were significantly elevated when compared with matched HCs [34-36]. The data presented here are consistent with these previous findings. Furthermore, our results highlight the close correlation between sTREM-1 and other clinical indicators, such as C3, IgG, and creatinine. We found that levels of sTREM-1 in serum were not only significantly different between SLE patients and HCs, but also obviously higher in active SLE patients than that of inactive group. The ROC curve of sTREM-1 revealed its probability as valuable biomarker. And all of the above results indicated that sTREM-1 has a high accuracy of predictive value in SLE.

TREM-1 is mainly expressed on myeloid cells, including a subset of monocytes, DCs, neutrophils, and macrophages. Herein, TREM-1 in PBMCs was screened as one of the hub genes and it was relevant to cytokines and type I IFN mediated responses in the pathogenesis of SLE based on high throughput analysis. Activation of TREM-1 in human monocytes was demonstrated to upregulate the expression of co-stimulatory molecules, leading to the differentiation of monocytes into immature DCs with subsequent improvement of the ability to elicit T-lymphocyte cell responses [22]. TREM-1-activated monocytes results in the production of multiple proinflammatory cytokines and chemokines [37]. Although numerous evidence highlighted pDCs as the major culprit to favor SLE development by secreting type I IFN [38, 39], as the most potent antigen presenting cells, mDC has attracted more and more researchers' attention. mDCs are considered as the prototype of conventional DCs (cDCs) and they play an active role in inducing both central and peripheral tolerance. In SLE, inappropriate presentation of self-antigens by mDCs to lymphocytes resulting in dysregulated autoreactive T cell and B cell activation [11, 40]. Our previous report provided the first evidence that the surface expression of TREM-1 on mDCs from spleen of MRL/*lpr* mice was enhanced when compared to wild type mice [23]. Nevertheless, the detailed roles and mechanisms of TREM-1 in mDCs and lupus remained elusive. TREM-1 was reported to be combined with TLR4 to synergistically promote the production of inflammatory cytokines in monocytes [41]. Our *in vitro* experiments revealed that either engagement of TREM-1 by its agonist or activation of TLR4 by LPS can affect the maturation and function of mDCs, which is manifested by the increased levels of CD40, TREM-1 and CCR7, enhanced chemotaxis and elevated inflammatory cytokines production. Of note, the agonistic monoclonal antibody of TREM-1 and LPS showed a synergistic effect only regarding the expression of CD40, rather than other molecules. The available data suggest that synergistic effects between TREM-1 and TLR4 might be not only cell type specific, but also functional specific.

Disorders of epigenetic processes give rise to several typical human autoimmune diseases. Altered miRNA profiles have been identified in patients with SLE and they are associated with immune disorders and organ damage [42, 43]. Accumulating studies demonstrate that miRNAs have the potential to be developed as therapeutic agents. For instance, Tfh cell overexpansion promotes autoimmune responses and disease flares in SLE. miR-21 is highly expressed in SLE $CD4^+$ T cells. Administration of Antagomir-21 significantly reduced the expansion of Tfh cells and improved intracellular iron homeostasis, contributing to the remission of disease symptoms in MRL/*lpr* mice [44]. In addition, miR-16 has a

potent protective role in relieving pathological symptoms in renal tissues and reducing proliferation of mesangial cells [45]. MiR-663 was found to impair the regulatory function of bone marrow-derived mesenchymal stem cells (BM-MSCs) by targeting TGF-β1. In MRL/*lpr* mice, inhibition of miR-663 could improve the remission of lupus [29]. Another study conducted by the same team showed that systemic delivery of miR-199a-5p agomir increased splenic $CD4^+$ T cell senescence through Sirt1/p53 pathway and alleviated lupus pathologies in MRL/*lpr* mice [46]. The above evidence supports the notions that manipulating specific miRNA expression *in vivo* can be novel therapeutic strategy for SLE.

Associated epigenetic regulatory mechanisms involved in TREM-1 cascade in mDCs remained unclear before. In this study, miRNAs that can target TREM-1 were predicted by bioinformatics analysis and we first identified miRNA-150-5p as one of the key regulators that inhibit TREM-1 expression by directly binding to its 3′ UTR in mDCs. Additionally, the dysregulated expression of miRNA-150-5p in spleen of lupus mice and PBMCs of SLE patients indicates that it participates in the pathological progression of lupus. These findings encouraged us to examine whether modulation of miR-150-5p could rescue autoimmune disorders in pristane-induced murine lupus. Our *in vivo* data indeed indicated that administration of miR-150-5p agomir successfully ameliorated disease phenotypes and restored immune homeostasis to some extent. Moreover, delivery of miR-150-5p agomir *in vivo* could also inhibit the over-activation of mDCs and suppress the expression and activation of TREM-1 in mDCs. One limitation of the present study is that we focused on mDCs, but other immune cells may be involved in TREM-1 regulation and controlled by miR-150-5p *in vivo*, which will be included in our future investigations.

As summarized in the graphical abstract, we have screened TREM-1 as one of the hub genes by bioinformatics analysis and demonstrated sTREM-1 as valuable clinical biomarkers. Moreover, we have verified the key roles of TREM-1 signal pathway in mDCs and lupus mice, and identified one pivotal factor, miR-150-5p, which was responsible for reduced inflammation in SLE by regulating over-activation of mDCs through NF-κB and STAT3 downstream of TREM-1 signal pathway. The *in vivo* data have shown that miR-150-5p agomir treatment ameliorated organ damage and autoimmune responses in lupus mice. Therefore, the current study advances our knowledge of the clinical significance of TREM-1 in SLE, and offers that miR-150-5p may serve as an effective therapeutic target for lupus.

Declarations

Ethical approval Informed consent was obtained from all human participants. All experiments were carried out in accordance with guidelines from the research committee at Wenzhou Medical University (Certificate No. SYXK- (Zhejiang, China) (2018-0017)). The study protocol was approved by the Clinical Research Ethics Committees of the First Affiliated Hospital of Wenzhou Medical University.

Consent to participate Informed consent was obtained from all subjects involved in the study.

Consent to publish Patients signed informed consent regarding publishing their data.

Availability of data and materials The data that support the fndings of this study are available from the corresponding author upon reasonable request. As such, the authors will follow guidance provided by the journal for sharing the data.

Conflict of interest The authors declare no competing interests.

Author contributions CH conceived the project and designed the experiments. CY collected and assembled data with help from SG, JY, TZ, ZX, YX, HQ, XZ, SL and AY. CH and CY prepared the first draft of the manuscript. LW, JW and CH supervised the work. All authors reviewed and approved the manuscript.

Funding This study was supported by National Natural Science Foundation of China (grant no. 81901660), Science and Technology Plan Project of Wenzhou (grant nos. Y20220389, Y20220045), and Zhejiang Province Natural Science Foundation (grant no. LTGY23H100001).

Abbreviations

SLE: Systemic lupus erythematosus; miRNAs: microRNAs; WT: wild type; HE: hematoxylin-eosin; IF: immunofluorescence; RT-PCR: Quantitative real-time reverse transcription-polymerase chain reaction; GAPDH: glyceraldehyde 3-phosphate dehydrogenase; DEGs: differentially expressed genes; PBMC: peripheral blood mononuclear cell; C3: complement 3; Ig: immunoglobulin; HC: healthy control; NC: negative control; SLEDAI: systemic lupus erythematosus disease activity index; ROC: receiver operating characteristic; AUC: area under the ROC curve; ELISA: Enzyme-linked immunosorbent assay; WB: Western blot; PAS: periodic acid-Schiff.

References

1. Kiriakidou M, Ching C L (2020) Systemic Lupus Erythematosus Ann Intern Med 172:ITC81-ITC96.http://dx.doi.org/10.7326/AITC202006020
2. Durcan L, O'Dwyer T, Petri M (2019) Management strategies and future directions for systemic lupus erythematosus in adults Lancet 393:2332-2343.http://dx.doi.org/10.1016/S0140-6736(19)30237-5
3. Schwartz N, Goilav B, Putterman C (2014) The pathogenesis, diagnosis and treatment of lupus nephritis Curr Opin Rheumatol 26:502-509.http://dx.doi.org/10.1097/BOR.0000000000000089
4. Murphy G, Isenberg D A (2019) New therapies for systemic lupus erythematosus - past imperfect, future tense Nat Rev Rheumatol 15:403-412.http://dx.doi.org/10.1038/s41584-019-0235-5
5. Chasset F, Francès C (2019) Current Concepts and Future Approaches in the Treatment of Cutaneous Lupus Erythematosus: A Comprehensive Review Drugs 79:1199-1215.http://dx.doi.org/10.1007/s40265-019-01151-8
6. Mackensen A, Müller F, Mougiakakos D, Böltz S, Wilhelm A, Aigner M, Völkl S, Simon D, Kleyer A, Munoz L, Kretschmann S, Kharboutli S, Gary R, Reimann H, Rösler W, Uderhardt S, Bang H, Herrmann M, Ekici A B, Buettner C, Habenicht K M, Winkler T H, Krönke G, Schett G (2022) Anti-CD19 CAR T cell therapy for refractory systemic lupus erythematosus Nat Med 28:2124-2132.http://dx.doi.org/10.1038/s41591-022-02017-5
7. Guo Q, Chen C, Wu Z, Zhang W, Wang L, Yu J, Li L, Zhang J, Duan Y (2022) Engineered PD-1/TIGIT dual-activating cell-membrane nanoparticles with dexamethasone act synergistically to shape the effector T cell/Treg balance and alleviate systemic lupus erythematosus Biomaterials 285:121517.http://dx.doi.org/10.1016/j.biomaterials.2022.121517
8. Szelinski F, Lino A C, Dörner T (2022) B cells in systemic lupus erythematosus Curr Opin Rheumatol 34:125-132.http://dx.doi.org/10.1097/BOR.0000000000000865
9. Dutertre C-A, Becht E, Irac S E, Khalilnezhad A, Narang V, Khalilnezhad S, Ng P Y, van den Hoogen L L, Leong J Y, Lee B, Chevrier M, Zhang X M, Yong P J A, Koh G, Lum J, Howland S W, Mok E, Chen J, Larbi A, Tan H K K, Lim T K H, Karagianni P, Tzioufas A G, Malleret B, Brody J, Albani S, van Roon J, Radstake T, Newell E W, Ginhoux F (2019) Single-Cell Analysis of Human Mononuclear Phagocytes Reveals Subset-Defining Markers and Identifies Circulating Inflammatory Dendritic Cells Immunity 51.http://dx.doi.org/10.1016/j.immuni.2019.08.008
10. Xiao Z X, Hu X, Zhang X, Chen Z, Wang J, Jin K, Cao F L, Sun B, Bellanti J A, Olsen N, Zheng S G (2020) High salt diet accelerates the progression of murine lupus through dendritic cells via the p38 MAPK and STAT1 signaling pathways Signal Transduct Target Ther 5:34.http://dx.doi.org/10.1038/s41392-020-0139-5
11. Liu J, Zhang X, Cao X (2022) Dendritic cells in systemic lupus erythematosus: From pathogenesis to therapeutic applications J Autoimmun 132:102856.http://dx.doi.org/10.1016/j.jaut.2022.102856
12. Crispín J C, Vargas-Rojas M I, Monsiváis-Urenda A, Alcocer-Varela J (2012) Phenotype and function of dendritic cells of patients with systemic lupus erythematosus Clin Immunol 143:45-50.http://dx.doi.org/10.1016/j.clim.2011.12.004
13. Gleisner M A, Reyes P, Alfaro J, Solanes P, Simon V, Crisostomo N, Sauma D, Rosemblatt M, Bono M R (2013) Dendritic and stromal cells from the spleen of lupic mice present phenotypic and functional abnormalities Mol Immunol 54:423-434.http://dx.doi.org/10.1016/j.molimm.2013.01.011

14. Gao S, Gong Y, Ji J, Yuan L, Han L, Guo Y, Fan X, Hou Y, Hua C (2017) A new benzenediamine derivative modulates Toll-like receptors-induced myeloid dendritic cells activation and ameliorates lupus-like syndrome in MRLlpr/lpr mice Eur J Pharmacol 803.http://dx.doi.org/10.1016/j.ejphar.2017.03.048
15. Denning N-L, Aziz M, Murao A, Gurien S D, Ochani M, Prince J M, Wang P (2020) Extracellular CIRP as an endogenous TREM-1 ligand to fuel inflammation in sepsis JCI Insight 5.http://dx.doi.org/10.1172/jci.insight.134172
16. Nguyen-Lefebvre A T, Ajith A, Portik-Dobos V, Horuzsko D D, Arbab A S, Dzutsev A, Sadek R, Trinchieri G, Horuzsko A (2018) The innate immune receptor TREM-1 promotes liver injury and fibrosis J Clin Invest 128:4870-4883.http://dx.doi.org/10.1172/JCI98156
17. Joffre J, Potteaux S, Zeboudj L, Loyer X, Boufenzer A, Laurans L, Esposito B, Vandestienne M, de Jager S C A, Hénique C, Zlatanova I, Taleb S, Bruneval P, Tedgui A, Mallat Z, Gibot S, Ait-Oufella H (2016) Genetic and Pharmacological Inhibition of TREM-1 Limits the Development of Experimental Atherosclerosis J Am Coll Cardiol 68:2776-2793.http://dx.doi.org/10.1016/j.jacc.2016.10.015
18. Wu Q, Zhou W, Yin S, Zhou Y, Chen T, Qian J, Su R, Hong L, Lu H, Zhang F, Xie H, Zhou L, Zheng S (2019) Blocking Triggering Receptor Expressed on Myeloid Cells-1-Positive Tumor-Associated Macrophages Induced by Hypoxia Reverses Immunosuppression and Anti-Programmed Cell Death Ligand 1 Resistance in Liver Cancer Hepatology 70:198-214.http://dx.doi.org/10.1002/hep.30593
19. Gao S, Yi Y, Xia G, Yu C, Ye C, Tu F, Shen L, Wang W, Hua C (2019) The characteristics and pivotal roles of triggering receptor expressed on myeloid cells-1 in autoimmune diseases Autoimmun Rev 18:25-35.http://dx.doi.org/10.1016/j.autrev.2018.07.008
20. Bouchon A, Facchetti F, Weigand M A, Colonna M (2001) TREM-1 amplifies inflammation and is a crucial mediator of septic shock Nature 410:1103-1107
21. Tammaro A, Derive M, Gibot S, Leemans J C, Florquin S, Dessing M C (2017) TREM-1 and its potential ligands in non-infectious diseases: from biology to clinical perspectives Pharmacol Ther 177:81-95.http://dx.doi.org/10.1016/j.pharmthera.2017.02.043
22. Pandupuspitasari N S, Khan F A, Huang C-J, Chen X, Zhang S (2016) Novel Attributions of TREMs in Immunity Curr Issues Mol Biol 20:47-54
23. Gao S, Yuan L, Wang Y, Hua C (2017) Enhanced expression of TREM-1 in splenic cDCs in lupus prone mice and it was modulated by miRNA-150 Mol Immunol 81:127-134.http://dx.doi.org/10.1016/j.molimm.2016.12.006
24. Hochberg M C (1997) Updating the American College of Rheumatology revised criteria for the classification of systemic lupus erythematosus Arthritis Rheum 40:1725
25. Gladman D D, Ibañez D, Urowitz M B (2002) Systemic lupus erythematosus disease activity index 2000 J Rheumatol 29:288-291
26. Huang R-Y, Yu Y-L, Cheng W-C, OuYang C-N, Fu E, Chu C-L (2010) Immunosuppressive effect of quercetin on dendritic cell activation and function J Immunol 184:6815-6821.http://dx.doi.org/10.4049/jimmunol.0903991
27. Lu M, Xu C, Zhang Q, Wu X, Tang L, Wang X, Wu J, Wu X (2018) Inhibition of p21-activated kinase 1 attenuates the cardinal features of asthma through suppressing the lymph node homing of dendritic cells Biochem Pharmacol 154:464-473.http://dx.doi.org/10.1016/j.bcp.2018.06.012
28. Ding C, Chen X, Dascani P, Hu X, Bolli R, Zhang H-G, McLeish K R, Yan J (2016) STAT3

Signaling in B Cells Is Critical for Germinal Center Maintenance and Contributes to the Pathogenesis of Murine Models of Lupus J Immunol 196:4477-4486.http://dx.doi.org/10.4049/jimmunol.1502043

29. Geng L, Tang X, Zhou K, Wang D, Wang S, Yao G, Chen W, Gao X, Chen W, Shi S, Shen N, Feng X, Sun L (2019) MicroRNA-663 induces immune dysregulation by inhibiting TGF-β1 production in bone marrow-derived mesenchymal stem cells in patients with systemic lupus erythematosus Cell Mol Immunol 16:260-274.http://dx.doi.org/10.1038/cmi.2018.1
30. Xu J, Qi Y, Xu W-H, Liu Y, Qiu L, Wang K-Q, Hu H-G, He Z-G, Zhang J-P (2016) Matrine derivate MASM suppresses LPS-induced phenotypic and functional maturation of murine bone marrow-derived dendritic cells Int Immunopharmacol 36:59-66.http://dx.doi.org/10.1016/j.intimp.2016.04.022
31. Shinde R, Hezaveh K, Halaby M J, Kloetgen A, Chakravarthy A, da Silva Medina T, Deol R, Manion K P, Baglaenko Y, Eldh M, Lamorte S, Wallace D, Chodisetti S B, Ravishankar B, Liu H, Chaudhary K, Munn D H, Tsirigos A, Madaio M, Gabrielsson S, Touma Z, Wither J, De Carvalho D D, McGaha T L (2018) Apoptotic cell-induced AhR activity is required for immunological tolerance and suppression of systemic lupus erythematosus in mice and humans Nat Immunol 19:571-582.http://dx.doi.org/10.1038/s41590-018-0107-1
32. Thomas C A, Tejwani L, Trujillo C A, Negraes P D, Herai R H, Mesci P, Macia A, Crow Y J, Muotri A R (2017) Modeling of TREX1-Dependent Autoimmune Disease using Human Stem Cells Highlights L1 Accumulation as a Source of Neuroinflammation Cell Stem Cell 21.http://dx.doi.org/10.1016/j.stem.2017.07.009
33. Cavaillon J-M (2009) Monocyte TREM-1 membrane expression in non-infectious inflammation Crit Care 13:152.http://dx.doi.org/10.1186/cc7882
34. Molad Y, Pokroy-Shapira E, Kaptzan T, Monselise A, Shalita-Chesner M, Monselise Y (2013) Serum soluble triggering receptor on myeloid cells-1 (sTREM-1) is elevated in systemic lupus erythematosus but does not distinguish between lupus alone and concurrent infection Inflammation 36:1519-1524.http://dx.doi.org/10.1007/s10753-013-9694-z
35. Bassyouni I H, Fawzi S, Gheita T A, Bassyouni R H, Nasr A S, El Bakry S A, Afifi N (2017) Clinical Association of a Soluble Triggering Receptor Expressed on Myeloid Cells-1 (sTREM-1) in Patients with Systemic Lupus Erythematosus Immunol Invest 46:38-47.http://dx.doi.org/10.1080/08820139.2016.1211140
36. Liu C-J, Tsai C-Y, Chiang S-H, Tang S-J, Chen N-J, Mak T W, Sun G-H, Sun K-H (2017) Triggering receptor expressed on myeloid cells-1 (TREM-1) deficiency augments BAFF production to promote lupus progression J Autoimmun 78.http://dx.doi.org/10.1016/j.jaut.2016.12.010
37. Haselmayer P, Grosse-Hovest L, von Landenberg P, Schild H, Radsak M P (2007) TREM-1 ligand expression on platelets enhances neutrophil activation Blood 110:1029-1035
38. Blanco P, Palucka A K, Gill M, Pascual V, Banchereau J (2001) Induction of dendritic cell differentiation by IFN-alpha in systemic lupus erythematosus Science 294:1540-1543
39. Baechler E C, Batliwalla F M, Karypis G, Gaffney P M, Ortmann W A, Espe K J, Shark K B, Grande W J, Hughes K M, Kapur V, Gregersen P K, Behrens T W (2003) Interferon-inducible gene expression signature in peripheral blood cells of patients with severe lupus Proc Natl Acad Sci U S A 100:2610-2615
40. Chan V S-F, Nie Y-J, Shen N, Yan S, Mok M-Y, Lau C-S (2012) Distinct roles of myeloid and

plasmacytoid dendritic cells in systemic lupus erythematosus Autoimmun Rev 11:890-897.http://dx.doi.org/10.1016/j.autrev.2012.03.004

41. Bouchon A, Dietrich J, Colonna M (2000) Cutting edge: inflammatory responses can be triggered by TREM-1, a novel receptor expressed on neutrophils and monocytes J Immunol 164:4991-4995
42. Hong S-M, Liu C, Yin Z, Wu L, Qu B, Shen N (2020) MicroRNAs in Systemic Lupus Erythematosus: a Perspective on the Path from Biological Discoveries to Clinical Practice Curr Rheumatol Rep 22:17.http://dx.doi.org/10.1007/s11926-020-00895-7
43. Zhang L, Wu H, Zhao M, Chang C, Lu Q (2020) Clinical significance of miRNAs in autoimmunity J Autoimmun 109:102438.http://dx.doi.org/10.1016/j.jaut.2020.102438
44. Gao X, Song Y, Du P, Yang S, Cui H, Lu S, Hu L, Liu L, Jia S, Zhao M (2022) Administration of a microRNA-21 inhibitor improves the lupus-like phenotype in MRL/lpr mice by repressing Tfh cell-mediated autoimmune responses Int Immunopharmacol 106:108578.http://dx.doi.org/10.1016/j.intimp.2022.108578
45. Qi H, Cao Q, Liu Q (2020) MicroRNA-16 directly binds to DEC2 and inactivates the TLR4 signaling pathway to inhibit lupus nephritis-induced kidney tissue hyperplasia and mesangial cell proliferation Int Immunopharmacol 88:106859.http://dx.doi.org/10.1016/j.intimp.2020.106859
46. Cheng T, Ding S, Liu S, Li Y, Sun L (2021) Human umbilical cord-derived mesenchymal stem cell therapy ameliorates lupus through increasing CD4+ T cell senescence via MiR-199a-5p/Sirt1/p53 axis Theranostics 11:893-905.http://dx.doi.org/10.7150/thno.48080

Supplementary Files

This is a list of supplementary files associated with this preprint. Click to download.

- Fig.S1A.pdf
- Fig.S1B.pdf
- SupplementaryTableS1.pdf
- SupplementaryTableS2.pdf
- SuplementryTableS3.xlsx
- SuplementryTableS4.xlsx
- SuplementryTableS5.xlsx
- SupplementaryTableS6.pdf